International Journal of Mechanical Sciences 82 (2014) 161–169

Contents lists available at ScienceDirect

International Journal of Mechanical Sciences

journal homepage: www.elsevier.com/locate/ijmecsci

Numerical analysis of thermomechanical phenomena influencing tool wear in finishing turning of Inconel 718

J. Díaz-Álvarez [a], J.L. Cantero [b], H. Miguélez [b,*], X. Soldani [b]

[a] Department of Bioengineering and Aerospace Engineering, University Carlos III of Madrid, Avenida de la Universidad 30, Leganés, 28911 Madrid, Spain
[b] Department of Mechanical Engineering, University Carlos III of Madrid, Avenida de la Universidad 30, Leganés, 28911 Madrid, Spain

ARTICLE INFO

Article history:
Received 3 September 2013
Received in revised form
1 March 2014
Accepted 7 March 2014
Available online 18 March 2014

Keywords:
Tool wear
Inconel 718
Numerical model
Wear modes

ABSTRACT

Inconel 718, one of the most used Ni alloys, is a low machinability material due to the elevated stresses and temperatures generated at the cutting edge during machining related to aggressive tool wear. The understanding of thermo-mechanical phenomena involved during cutting is required for enhancement of wear performance. In this work a three dimensional (3D) numerical model based on finite element (FE) is applied for simulation of dry turning of Inconel 718. Despite the elevated computational cost, 3D modeling is required for analysis of wear mechanisms. The model was validated with turning tests. Main wear modes experimentally identified (chipping, notching, built up edge BUE) were related to variables predicted using the numerical model, such as temperature and plastic strain at the chip. Good correlation between experiments and numerical results was observed, and strong influence of the side cutting edge in wear performance was found.

1. Introduction

Nickel alloys owe excellent mechanical properties at high temperature and elevated corrosion resistance and are widely used in high responsibility applications. Machining of Ni alloys is still a challenge due to the aggressive conditions of cutting affecting surface state and tool wear evolution [1]. Wear patterns induced in cutting tools are due to the combined effect of different wear mechanisms involved in sliding friction occurring at the contact interface between tool, chip and machined surface [2].

The trend to experience elevated strong work hardening is an inherent characteristic of Ni alloys directly related to surface integrity and tool wear. Highly deformed material at the machined surface presents elevated hardness and residual stress affecting service life of the component [3,4]. Plastic deformation is related to generation of residual stresses and microhardness enhancement [5]. Also extremely elevated temperature at the cutting edge and adjacent zones are generated, affecting tool wear. These aggressive conditions have motivated the exploration of more efficient coolants like N_2 for cryogenic machining of Ni alloys [6].

It is common to observe notching, being a significant failure mode during machining Ni alloys. Notch formation results from combining different mechanisms. The work-hardened layer has been considered as the most important cause of notching when machining Ni alloys. Flank wear, chipping, BUE and catastrophic failure also cause tool rejection during machining of Ni alloys [1]. Burr formation commonly occurs as a consequence of work hardened layer, usually leading to catastrophic breakage of the insert edge.

Different authors have focused their attention on tool wear analysis when machining Ni alloys, most of them developing experimental work valuable for understanding of wear mechanisms and surface state; a review of recent advances can be found in [7]. Also attempts in numerical modeling have been made in order to analyze factors affecting wear evolution. Simulations have demonstrated their ability to improve the understanding of wear mechanism and surface state giving information about difficult to measure variables during cutting.

Despite the limitations of two dimensional (2D) modeling, this approach has been extensively used for simulation of machining for decades. Concerning wear analysis, it was presented in [8] a 2D finite element tool wear model able to predict the worn geometry quantitatively in cemented carbide tool machining nickel-based alloys. The influence of different wear and friction models on parameters affecting the wear progression was investigated. It was demonstrated that the friction model has a major influence on the simulated wear profile, by influencing the relative velocity.

The need to reproduce the complex tool geometry in tool wear analysis requires the development of three dimensional (3D) approaches. It is worth noticing the importance of proper prediction of the location of each type of wear (for instance notching, occurring at the intersection between cutting edge and free

* Corresponding author.
E-mail address: mhmiguel@ing.uc3m.es (H. Miguélez).

http://dx.doi.org/10.1016/j.ijmecsci.2014.03.010
0020-7403/

surface of the worpiece). When 2D modeling is developed it is not possible to distinguish between different areas in the cutting edge.

Main drawback of the 3D modeling is the elevated computational cost especially when small elements are required; however recently efforts have been made in the application of this modeling technique to the analysis of wear. Main contributions are commented below highlighting those related to modeling of Ni alloys machining.

Aurich and Bill [9] presented an early work in 3D finite element (FE) modeling of machining operations with segmented chip formation. Two different methods, shear localization due to thermal softening and crack initiation and propagation, were utilized for the simulation of chip segmentation.

Computational modeling of 3D turning process of steel alloy AISI 4340, in the presence of variable design inserts, was studied in [10]. The temperature and stress distributions and tool wear contours revealed the advantages of variable edge micro-geometry design.

3D finite element modeling was utilized to predict chip formation, forces, temperatures and tool wear on multi-layer coated inserts in turning Ti–6Al–4V [11]. The temperature distributions and tool wear contours demonstrated some advantages of coated insert.

Attanasio et al. [12] focused on the 3D numerical prediction of tool wear implementing an analytical model, able to take into account the diffusive wear mechanism. Furthermore, an advanced approach to the model of heat transfer phenomena at the tool–chip interface was included in the numerical simulation. The simulation strategy gave the possibility to properly evaluate the tool wear. 3D FEM results were compared with some experimental data obtained by turning AISI 1045 steel using uncoated WC tool and good agreement was found out.

Özel and Ulutan [13] developed 3D FE simulations in order to predict machining induced residual stresses in Ti–6Al–4V and IN100 alloys, comparing numerical results with experiments. It was shown the influence of the tool micro-geometry in residual stresses: they become more compressive with increased edge radius but more tensile at the surface when coated.

Rotella et al. [14] proposed a 3D FE model for studying the turning process of AA7075-T651 alloy in terms of grain size and hardness prediction. The Zener–Hollomon parameter was employed for relating the deformation conditions to the recrystallized grain size while the Hall–Petch equation was employed for the hardness; the simulation results were validated with experimental data from performed tests. The numerical results showed a good prediction of the micro-structural changes occurring during machining of the workpiece. 3D approach was required to observe the effect of tool nose radius in the machined surface and subsurface integrity.

Uhlmann et al. [15] developed a realistic simulation of the chip formation in orthogonal machining of Inconel 718 using 2D and 3D FE simulation in order to compare chip morphology obtained with both approaches. Good correlation was found between 2D and 3D predictions and the experiments.

Turning of Inconel 718 was simulated in [16] using experimentally determined mechanical properties at elevated strain rates and temperatures. The cutting forces predicted by the FE models showed good agreement with experimentally measured data. The simulation was not able to predict chip morphology due to the lack of a suitable sub-routine to properly define the onset and propagation of shear localization and fracture along the shear plane.

Not only finite element method has been used in the numerical modeling of machining. Lazoglu and Islam [17] recently presented a 3D temperature prediction model using finite difference approach for the oblique machining processes. Finite difference method, selected in order to solve the heat transfer problem, is computationally much faster compared to finite element models. The authors simulated 3D temperature fields in oblique machining in the order of minutes comparing to hours or days in FE simulations.

Illoul and Lorong [18] worked on the 3D implementation of the constrained natural element method (CNEM) in order to simulate material forming and machining, involving large strains. The CNEM is a member of the large family of mesh-free methods, but it is at the same time very close to the finite element method.

The main objective of this paper is to analyze variables related to wear evolution in finishing turning of Inconel 718 using 3D numerical modeling based on the FE method. As was explained previously 3D approach is required to simulate the different zones of the cutting edge. This is especially important when small depth of cut is involved (as is the case of finishing turning) where the influence of tool nose is significant. Despite the interest of the results provided in the scientific literature no information was found concerning the 3D numerical analysis of the thermo-mechanical phenomena influencing wear patterns when turning Inconel 718. The analysis of notching, being one of the most important wear modes when machining Inconel 718, implies the use of 3D approach in order to model the whole cutting edge. Tool wear evolution of different inserts in finishing turning of Inconel 718 was studied in a recent work of the authors using an experimental approach [19]. Different coupled wear mechanisms were observed being especially significant in chipping and notch wear due to high work hardening of the Ni alloy. Also built up edge (BUE) was observed when adhesion was promoted by insert configuration. Strong influence of the side cutting edge angle κ_r in the wear evolution and tool life has been observed from experimental analysis: increasing κ_r diminishes the cutting aggressiveness for the tool. In this work 3D numerical modeling is applied with the aim of reproducing and analyzing thermo-mechanical variables influencing tool wear obtained in the workpiece.

2. Numerical modeling

A three dimensional model of turning was developed using an updated Lagrangian software (DEFORM-3D) in which chip separation from workpiece was achieved with continuous remeshing. DEFORM is a special purpose code commonly used in the literature for cutting simulation.

Fig. 1a shows the deformed mesh of the 3D model including boundary conditions. The workpiece was modeled as a prismatic piece of Inconel 718 and the effect of the curvature of the workpiece was neglected. The cutting parameters, typical in finishing turning operations, were: feed rate 0.1 mm/rev and depth of cut 0.5 mm and cutting speed ranged between 50 and 400 m/min.

The tool reproduced exactly the geometry and cutting conditions of the inserts used in the turning tests those are described in the next section. Fig. 1b shows the detail of insert geometry (tip angle is 80°). It is important to reproduce exactly the edge radius and tool tip shape because of the influence of the tool geometry on thermomechanical phenomena induced during cutting [20].

The tool was modeled with a rake angle of 17° and a clearance angle of 7° respectively. It is worth noting that the geometry of the tool was slightly modified in order to take into account the phenomenon of variation of geometry occurring at the first stage of machining with new tool. It was found in the literature evidence about the generation of a sudden flank wear which occurs in few cutting instants. The machining tests used for model validation were performed during a period of time large enough to observe this phenomenon. The experimental evidences from turning tests carried out with new insert, showed also in the present work, that

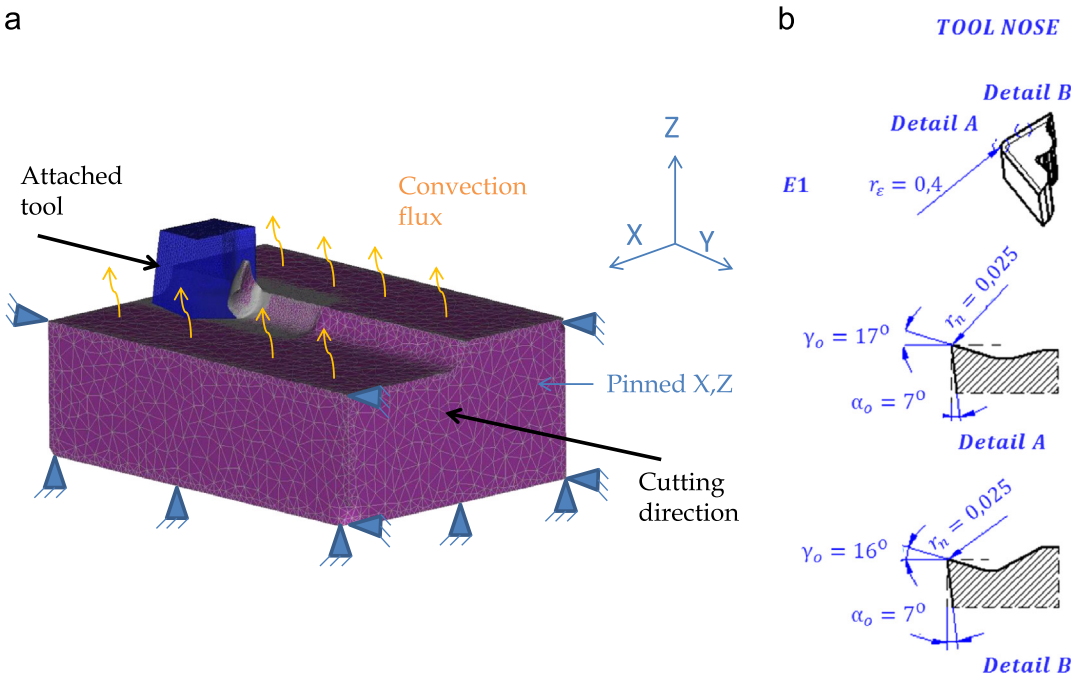

Fig. 1. a) Configuration of the numerical model. b) Edge configuration (courtesy by SECO).

the tool underwent a sudden wear when machining started. The initial average flank wear observed was around 0.050 mm, coincident with the value observed in the work of Filice et al. [21], reporting the same phenomenon. Physical properties of the tool material available in the code DEFORM for carbide tool [22] are summarized in Table 1.

Concerning boundary conditions, the contour of the tool was fixed and the workpiece moved at the cutting speed while the displacements out of the direction of the cutting speed are constrained at the bottom.

The angle between the cutting edge line and the longitudinal axis of the tool, side cutting edge angle (κ_r according to International Standard Organization ISO 3685, see Fig. 2a), influences tool performance during machining of Ni alloys. When κ_r is increased the length of the edge in contact with the workpiece is larger and stresses and temperatures are diminished in consequence, since the forces and heat are distributed over a larger portion of the cutting edge. The inserts were positioned with two different values of κ_r in order to analyze the influence of this parameter, also analyzed in experimental tests (see the next section).

The behavior of workpiece material was modeled using the constitutive equation of Johnson–Cook available in the code DEFORM for Inconel 718:

$$\sigma_Y = (A + B\varepsilon_p^n)\left(1 + C\ln\frac{\dot{\varepsilon}_p}{\dot{\varepsilon}_0}\right)\left(1 - \left(\frac{T - T_0}{T_m - T_0}\right)^m\right) \quad (1)$$

where σ_Y is the tensile flow stress, ε_p is the cumulated plastic strain, $\dot{\varepsilon}_p$ is the equivalent Mises plastic strain rate and T is the absolute temperature. The parameters of Eq. (1) are summarized in Table 2 [22]. Strain hardening, strain rate hardening and thermal softening are accounted. Physical properties of Inconel are provided in Tables 3–6 [22].

Contact at the interface was modeled with a constant friction coefficient equal to 0.8; this value is in the order of the coefficients used in other 3D and 2D models of metal cutting (see for instance [23–25]. Despite the simplicity of Coulomb model it is commonly used in machining models being able to reproduce sticking phenomena when high enough value of friction coefficient is implemented [8,23,24].

Table 1
Properties of the tool (WC) [22].

Tool (WC)	
Thermal conductivity – 293 K – (W/m/K)	59
Specific heat capacity (J/kg K)	15
Thermal expansion (/K)	$5.6 \times 10-6$
Tool convection (W/tw1 m2/K)	0.03
Density (kg/m3)	12
Poisson ratio	0.3
Modulus of -1 elasticity (GPa)	650

Thermal contact at the interface tool/chip was established with negligible thermal resistance in order to reproduce the conditions induced by extreme pressures and adhesion between chip and tool. In the paper it is assumed that the totality of the frictional energy is transformed into heat. The proportion of the frictional heat energy allocated to the chip is characterized by the coefficient of heat partition. A detailed analysis of the contact mechanics at the scale of surface asperities would be needed to characterize the value of the coefficient along the sliding zone; however this is not the scope of the present work. The value of heat partition coefficient equal to 0.5 (50–50%) is commonly adopted in the literature and has been assumed in previous works of the authors [23,24]. This assumption is also coherent with the sound work of Grzesik and Nieslony [26] where the heat partition coefficient was found to be between 0.42 and 0.68, for different tools coated and uncoated when machining stainless and carbon steel. The variation with the Peclet number ($Pe = \frac{l_c V_{ch}}{\alpha_T}$, where l_c is the contact length, V_{ch} is the sliding velocity of the chip and α_T is the tool material diffusivity) is not strong and the assumption of heat partition coefficient equal to 0.5 seems reasonably for the present work in the absence of more precise information. Thus, along the sliding zone, frictional heat is equally allocated to the two bodies in contact.

Convection to air was simulated in the free surfaces of the workpiece and the tool (see Fig. 1a) although the characteristic time of this phenomenon is large compared to the simulated cutting time. Heat conduction is allowed in the workpiece and tool

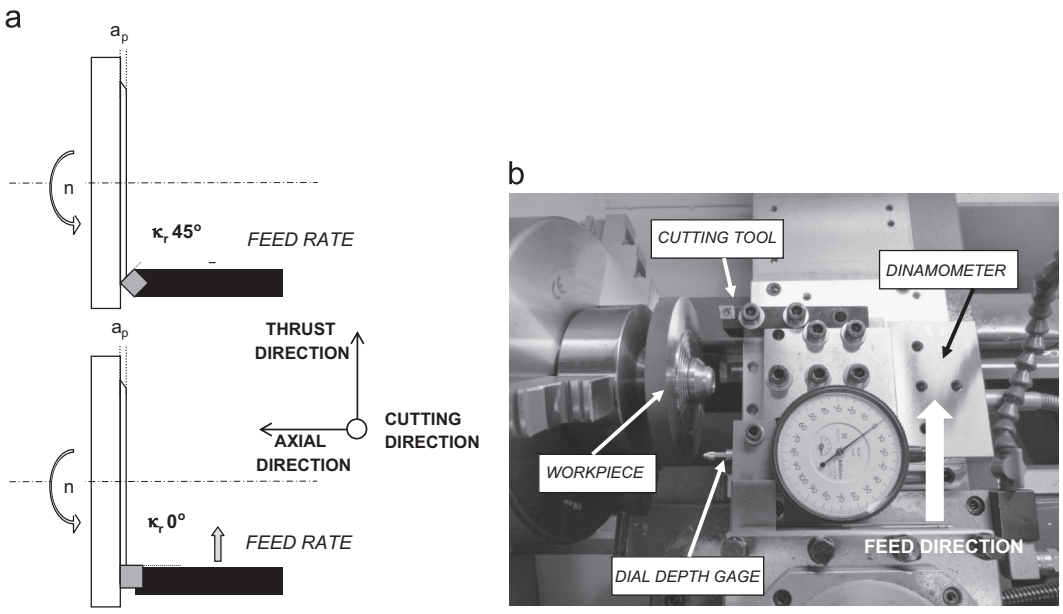

Fig. 2. Experimental stand: a) scheme of κ_r during turning tests; b) configuration of experimental device showing tool position and cutting direction.

Table 2
Parameters of constitutive equation for Inconel 718 [22].

A (MPa)	B (MPa)	n	c	m	$\dot{\varepsilon}_o$(1/s)	T_m (K)
790	610	0.23	0.011	3.28	0.01	1573

Table 3
Physical properties of the workpiece.

Inconel 718	
Workpiece convection (W/m^2/K)	0.08
Density (kg/m^3)	8.2
Poisson ratio	0.3
Modulus of elasticity – 293 K – (GPa)	217

Table 4
Temperature dependence of thermal conductivity for Inconel 718 [22].

Thermal conductivity (W/m/K)	
293 K	10.31
373 K	11,88
473 K	13,6
673 K	16,6
873 K	20,1
1073 K	26,3
1573 K	30,75

Table 5
Temperature dependence of specific heat capacity for Inconel 718 [22].

Specific heat capacity (J/kg K)	
293 K	362
373 K	378
473 K	400
673 K	412
873 K	460
1073 K	544
1573 K	583

Table 6
Temperature dependence of thermal expansion for Inconel 718 [22].

Thermal expansion (/K)	
293 K	1.20×10^{-5}
373 K	1.31×10^{-5}
473 K	1.35×10^{-5}
673 K	1.41×10^{-5}
973 K	1.58×10^{-5}

and the boundaries are far enough to ensure that they remain at the room temperature during the simulation.

The mesh of the workpiece is refined at the zone around the cutting edge. Despite the interest of the information that can be obtained from numerical modeling one of the most important limitation is the influence of mesh size. The mesh was rough far from the contact zone and much finer at the zone close to the interface (around 10 μm). Whole mesh needed approximately 150,000 elements for the workpiece and 120,000 elements for the tool. A sensibility analysis was developed concerning the effect of the element size. Evolution of machining forces with element size in the range 10–30 μm showed low influence in the forces, differences being lower than 10%. Element size was stated equal to 10 μm being a compromise between accuracy and computational efficiency.

3. Experimental work and model validation

Finishing turning tests were developed in a lathe Pinacho Smart turn 6/165; cutting forces were measured with a dynamometer Kistler 9257B for model validation. The workpiece was Inconel Alloy 718 annealed 968 °C held for 50 min, water cooled, shaped as a disc with diameter 150 mm and thickness 20 mm. Position of the tool and tool displacement direction, at constant cutting speed, is indicated in Fig. 2b. The longitudinal tool axis was

positioned parallel to the lathe axis. An experimental device based on a precise dial depth gage (Mitutoyo ref. 3109, resolution 0.001 mm) was installed in the lathe, allowing the measurement of effective depth of cut in each pass. The objective was to avoid the uncertainty in the establishment of the depth of cut especially significant when a small value of depth is considered (0.5 mm in this case).

Commercial carbide diamond shaped cutting inserts for finishing operation (tool manufacturer Seco, [27]) were selected. The inserts were horizontally positioned on the tool holder, owing tip angle equal to 80° and tip radius equal to 0.4 mm. Tool material was based on carbide TS2000 recommended by the tool manufacturer for finishing operations of low machinability alloys. The insert was coated with a multilayer coating (inner layer TiAlN and external layer TiN), suitable for machining of thermo-resistant alloys. Although uncoated carbide tools are also suitable for machining Inconel 718 [28], in general the use of proper coating enhances the wear behavior of the inserts.

As it was commented in the previous section, tool geometry, shown in Fig. 1b, was slightly modified in order to account for the sudden flank occurring at the initial instant of the turning tests, observed both at the experiments of this work and in the scientific literature [21]. The inserts were positioned with two different values of κ_r (0° and 45°) corresponding to numerical simulations (Fig. 2a).

Turning tests were carried out at 50, 70, 100 and 400 m/min. Cutting velocities 50 and 70 m/min are in the range recommended by the tool manufacturer for finishing turning of Inconel 718 thus the analysis of wear evolution is applicable to industrial operations. Tool wear evolution was analyzed for the velocities 50 and 70 m/min and the details were published in a previous work of the authors [19]. In the next section the wear mechanisms observed are related to the numerical results obtained with the model. The upper values 100 and 400 m/min were tested in order to observe the evolution of numerical results with cutting speed. The analysis of wear evolution at high velocity has not been carried out since the range of recommended cutting speed is much lower and the wear performance of the inserts at high velocities is dramatically reduced.

Validation was performed comparing numerical and measured experimental forces. Figs. 3a and b shows cutting force F_c, thrust force F_t and axial force F_a for all cases analyzed. Good accuracy is observed for cutting force (for cutting edge angle 0° and 45° respectively). As it is commonly observed cutting forces decreased with cutting speed as a consequence of thermal softening [23,24].

The accurate prediction of thrust force requires fine meshes commonly leading to very long simulation time even in the case of two dimensional approaches. Models based in 2D approach with a fine mesh allow good prediction of thrust force (see for instance a recent work of the authors focusing on modeling orthogonal cutting of Ti alloy [29]).

In the present paper a compromise between accuracy and computational cost has been reached: although thrust force and axial force are not so accurate predicted as cutting force (see Fig. 3a and b), the error (ranging from 0% to 25%) is lower than that obtained in other recent works dealing with 3D modeling of cutting of different alloys (see for instance the work of Haddag and Nouari [30] showing errors around 50% in predicted thrust force in turning of AISI 1045; or the paper of Ozel and Ulutan [25] reporting errors between 20% and 45% when predicting thrust and feed force in turning of Ti alloy). Significant influence of the sudden flank was observed when comparing the results with the simulations carried out with the nominal geometry of the insert without initial flank wear. When no initial wear is considered maximum errors around 50% in thrust force are observed, while the influence in cutting force was almost negligible. It is worth to note the importance of accounting for the sudden flank phenomenon when modeling metal cutting with a 3D approach. All numerical results included in this paper were obtained with the model considering the initial wear.

4. Results and discussion

The paper focuses on thermo-mechanical phenomena occurring at the work piece, influencing tool wear mechanisms. The model was used for prediction of variables related to tool wear evolution: contact length, chip temperature and equivalent. These variables were obtained from machined workpiece; thus it was necessary to stabilize cutting process. The time required for stabilization of these variables at the workpiece is much more reduced than that required to reach steady state conditions at the cutting tool. The models reproducing tool wear evolution requires steady state of temperature at the tool, sometimes requiring an artificial mechanism to accelerate attainment of thermal steady state, such as the approach described in [31]. However this is not the aim of the present work. The paper focuses on the thermo-mechanical phenomena occurring at the workpiece due to the nature of the material (for instance the strain hardening capability) and the relation of the predicted variables with the observed wear mechanisms during turning experiments, depending on cutting conditions.

Values of temperature were obtained at the chip at different locations along the cutting edge such as at the tool nose, in the middle zone of the edge and close to the notch zone (the intersection between the cutting edge and the machined surface). It is important to note that the temperature in the chip is not the same as the temperature reached at the tool when steady state conditions are reached. As it has been commented previously, the computational cost of 3D modeling leads to very large calculation time. The qualitative information given by the chip temperature is important to compare between different configurations of the tool or between cutting conditions; however it does not provide

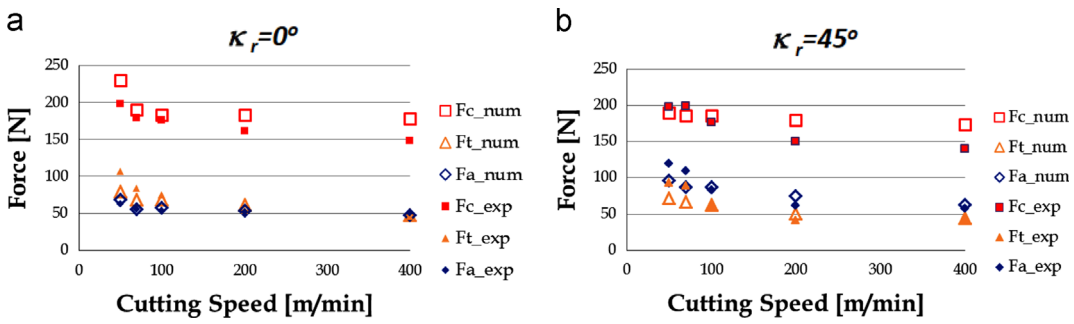

Fig. 3. Numerical and experimental cutting force F_c , thrust force F_t and axial force F_a a) κ_r=0°; b) κ_r=4°.

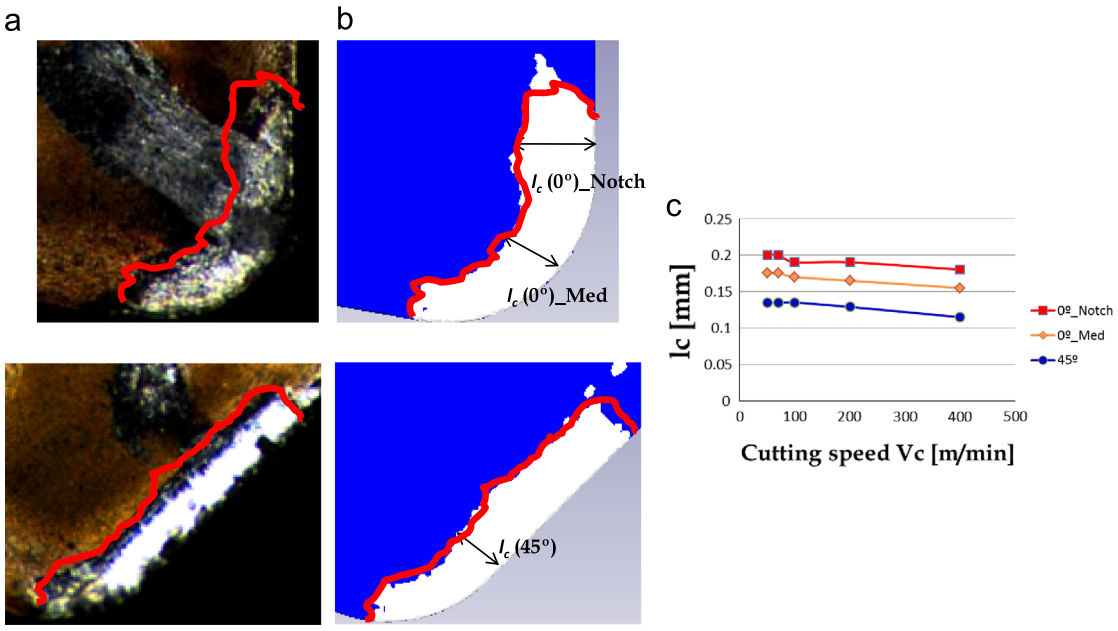

Fig. 4. a) Contour of the contact area at the rake surface (highlighted with an auxiliar line) obtained after cutting time 1.5 min at cutting speed 50 m/min (above $\kappa_r = 0^\circ$ and below $\kappa_r = 45^\circ$) b) Estimation of contact length l_c from numerical simulations: view of contact zone (light color corresponds to normal pressure > 0), and the same lines used in the photographs are superimposed to the contact zone contour. c) Prediction of evolution of l_c with cutting speed for $\kappa_r = 45^\circ$ (constant along the cutting edge) and $\kappa_r = 0^\circ$ (mean value at the cutting edge and at the notch zone).

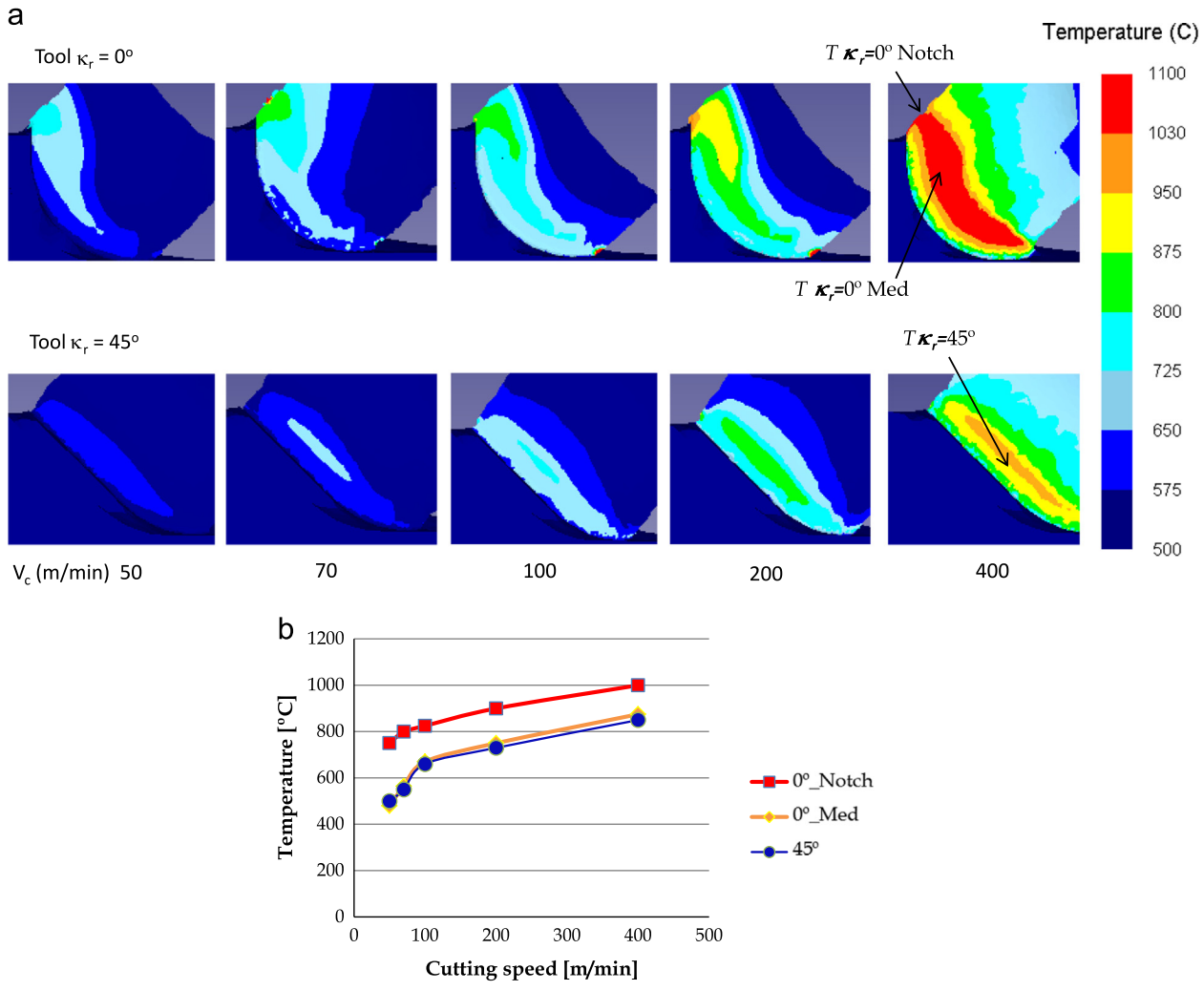

Fig. 5. Evolution with cutting speed of chip temperature T: a) view of temperature fields at the interface tool/chip ; b) Maximum temperature at three different zones considered vs cutting speed.

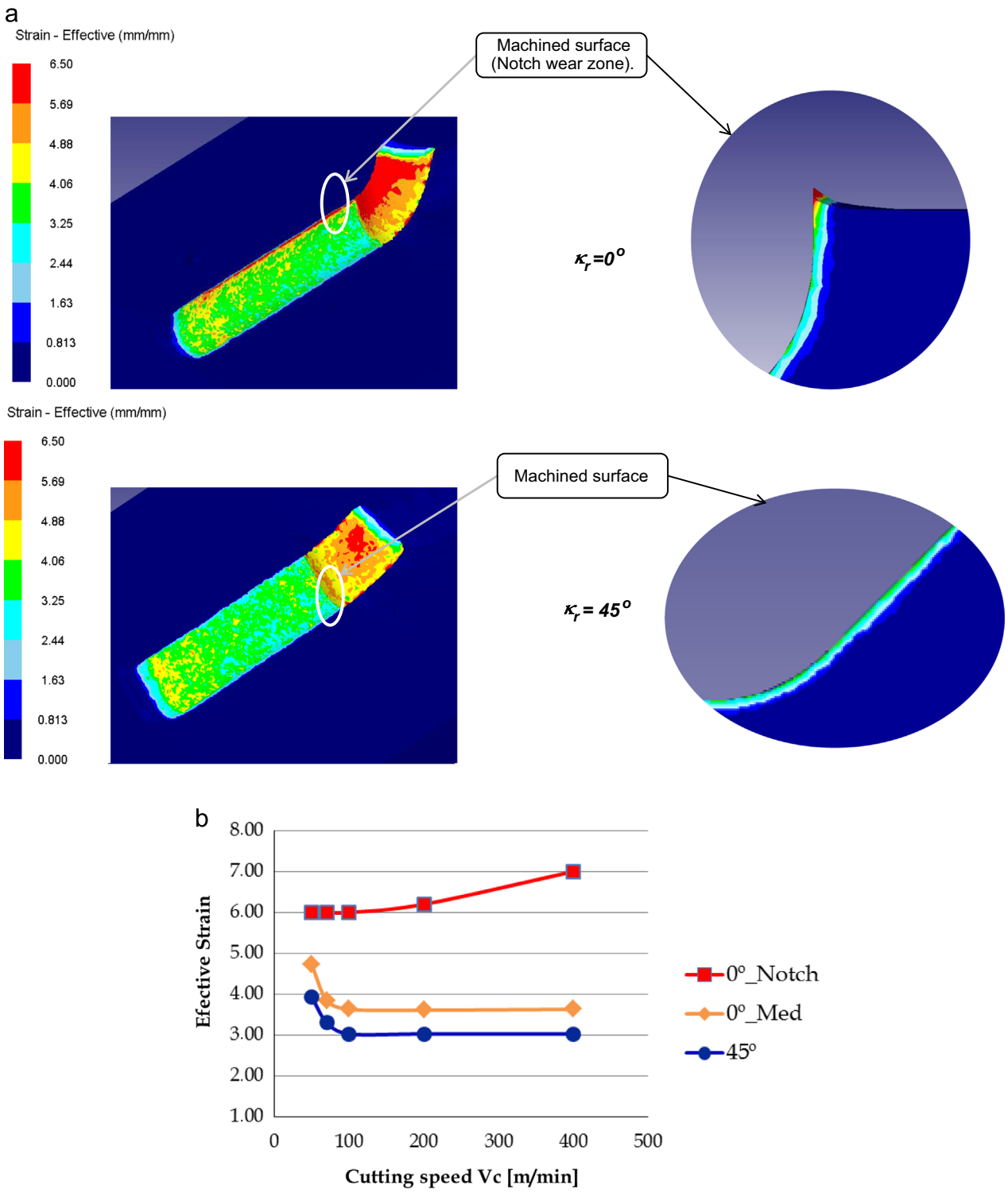

Fig. 6. Effective plastic strain during cutting a) κ_r =0° and κ_r=45° (cutting speed 70 m/min); b) evolution of effective plastic strain at three different zones considered vs cutting speed.

quantitative information about the temperature at the tool. Plastic strain was obtained at different points of the machined surface close to the middle zone of the edge and close to the notch zone.

Tool-chip contact length l_c was obtained from simulations considering the contact area that is the zone where normal stress is higher than zero. The predicted contact area was compared with the shape and extension of the zone were coating is removed at the rake surface of the insert. Fig. 4a shows the images of rake surface obtained after cutting time equal to 1.5 min (cutting speed 50 m/min, κ_r=0° and 45°) corresponding to moderate level of wear. The predicted contact area for the same cutting conditions is presented in Fig. 4b showing good correlation with experiments.

In the cases corresponding to side cutting edge angle κ_r=45° it was observed a constant value of l_c along the cutting edge; thus this value is provided in Fig. 4c, giving the evolution of l_c with cutting speed. However in the cases corresponding to side cutting

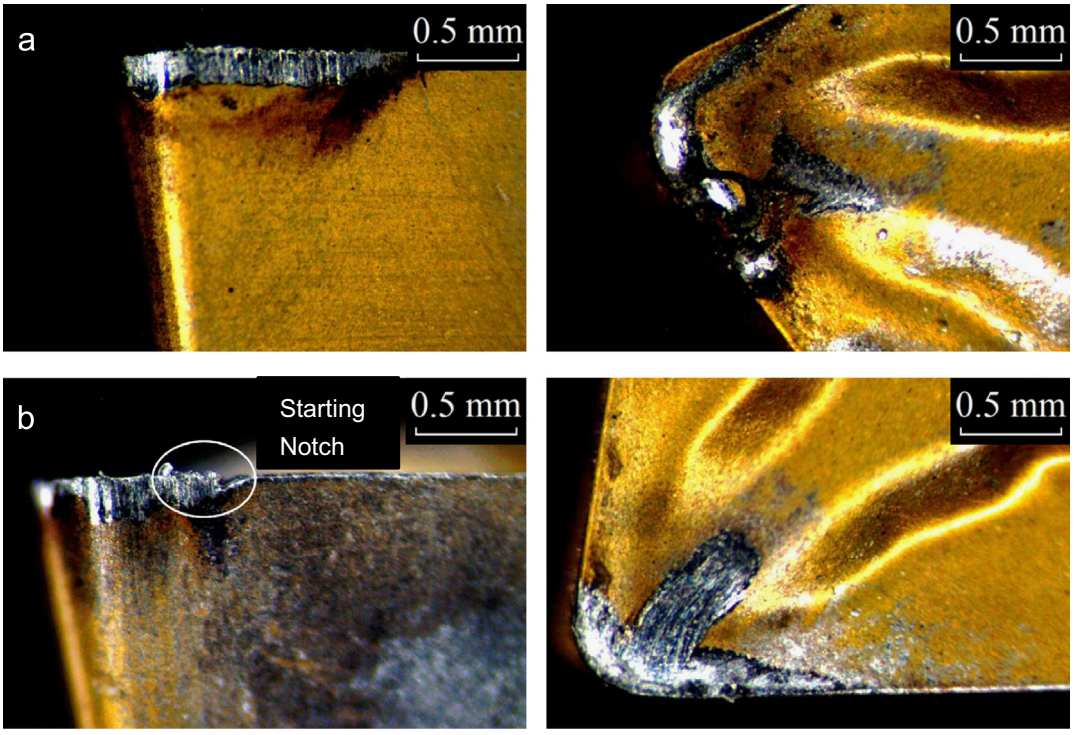

Fig. 7. View of cutting inserts (cutting speed 50 m/min, cutting time 4 min) a) with $\kappa_r=45^\circ$ showing flank wear ; b) with $\kappa_r=0^\circ$ showing notch onset and BUE.

edge angle $\kappa_r=0^\circ$ the contact length is larger at the zone where the notch is generated (outer zone of the depth of cut, Fig. 4b). Evolution of the contact length at the notch zone and the mean value at the edge are presented in Fig. 4c.

Concerning the differences observed in l_c for $\kappa_r=0^\circ$ and 45° they are due to the different effective undeformed chip thickness (lower for the insert with $\kappa_r=45^\circ$). According to Toropov and Ko [32] the ratio between contact length l_c and the undeformed chip thickness a can be estimated (for a wide collection of metallic materials) as $(l_c/a)=2.05\xi-0.55$, being ξ the chip thickness coefficient equal to the ratio between the chip thickness and the undeformed chip thickness ($\xi=a_1/a$). This coefficient mainly depends on the friction coefficient, cutting angles and edge radius. Since these parameters are the same in all tests performed it is reasonable to assume that contact length is proportional to the undeformed chip thickness and thus predicted contact length is lower for the case of $\kappa_r=45^\circ$.

Contact length decreases slightly with cutting velocity as has been shown in previous work [24]. This behavior is related to the increment of normal pressure as the cutting speed increases related to enhanced aggressiveness for the cutting tool.

The evolution with cutting speed of chip temperature fields is shown for $\kappa_r=0^\circ$ and 45° in Fig. 5a. Maximum temperature was obtained at three different locations at the elements of the chip in contact with the cutting edge. Chip temperature is more or less constant along the cutting edge for the insert with side cutting edge angle κ_r equal to 45°, while the level of temperature is approximately uniform along the cutting edge for $\kappa_r=0^\circ$, but it is significantly increased at the notch zone.

This behavior could be related to the enhanced aggressiveness and the trend to generate notch when the angle κ_r is small, as was demonstrated in a previous work of the authors [19]. The temperature increases with cutting speed (see Fig. 5b). As it was commented before, the temperature is obtained at the deformed workpiece for a large enough cutting time ensuring stabilized temperature at the chip. However the cutting time is not large enough to reach thermal steady state conditions in the tool. It is really difficult to stabilize temperature at the tool because of the large computational time required. It was shown in a previous work of the authors [24] that the chip temperature controls the nature of the tool–chip contact (sliding vs sticking) by tuning the level of the flow stress of the work-material (thermal softening). An increase of temperature leads to a decay of the flow stress that favors sticking contact. Thus the enhanced temperature at the chip affects the wear mechanisms directly related to temperature (such as diffusion) and also those related to workpiece material adhesion resulting in BUE.

Fig. 6a compares the fields of equivalent plastic strain for $\kappa_r=0^\circ$ and 45° (cutting speed 70 m/min); similar figures were obtained in the rest of cases analyzed. Deformation is significantly higher close to the notch zone in the case $\kappa_r=0^\circ$. It is possible to observe small burr acting over the insert at the zone where the notch is generated. High temperature at the workpiece together with a heavily work hardened characterized by high level of strain corroborates the theories explaining notch formation. Moreover deformation is higher in the medium zone of the edge for $\kappa_r=0^\circ$ tan for $\kappa_r=45^\circ$ leading to enhanced abrasion and in consequence accelerating tool wear for $\kappa_r=0^\circ$. The equivalent plastic strain along the cutting edge decreases slightly with cutting speed from 50 to 70 m/min and remains constant for further increments of cutting speed; however deformation increases at the notch for the case $\kappa_r=0^\circ$ (see Fig. 6b). The strain hardening capability of the Ni alloy is moderated by the thermal softening enhanced by the increment of cutting speed.

Numerical results presented in Figs. 4–6 could be related to the onset and evolution of wear observed when machining with the inserts $\kappa_r=0^\circ$ and $\kappa_r=45^\circ$ [19]. The type of wear observed at the beginning of the tool wear turning tests under dry conditions corresponds to the fresh tool geometry and conditions assumed during the numerical modeling described above. The inserts were tested without coolant at cutting speeds 50 and 70 m/min; those are in the range recommended by the tool manufacturer.

The angle $\kappa_r=0^\circ$ led to aggressive conditions for the cutting edge as illustrated in Fig. 7a and b, showing worn tools ($\kappa_r=0^\circ$ and

45°) after cutting time 4 min at cutting speed 50 m/min. The state of the tool $\kappa_r=0°$ shows more deteriorated state with notching initiation. The insert with angle $\kappa_r=0°$ showed initiation of chipping, notch and BUE (built up edge) at the beginning of the tests, both at 50 (Fig. 7) and 70 m/min. The progression of chipping and notch was significantly higher for cutting speed 70 m/min, probably due to the enhanced temperature at higher velocity. Also contact length decreases for higher cutting speed, promoting higher pressure and cutting edge deterioration. Also significant flank wear was identified leading to termination of tool life (9 min) for cutting speed 50 m/min. Flank wear also appeared for cutting speed 70 m/min; however the reduced tool life in this case did not allow reaching significant levels of flank wear. Although final edge breakage due to chipping was observed at 70 m/min, notch wear progressed rapidly.

5. Conclusions

Tool wear mechanisms of coated carbide inserts involved in finishing turning of Inconel 718 have been analyzed using a numerical approach. A 3D model has been developed using the commercial code DEFORM 3D reproducing accurately geometry and cutting conditions involved in experimental tests performed under dry conditions. The sudden flank wear, which occurs in few cutting instants during turning tests, was taken into account in the model. Better prediction of thrust force when compared with the value obtained with the nominal geometry of the tool was achieved. Numerical modeling allowed the analysis of thermo-mechanical phenomena involved in tool wear mechanisms.

Numerical modeling demonstrated the influence of side cutting angle κ_r on tool performance. Enhanced temperature and work hardening led to aggressive conditions for the case $\kappa_r=0°$. This effect was observed along the cutting edge originating flank wear and especially at the zone experiencing notch wear.

Also the trends with cutting speed are observed in the range 50–400 m/min. Increasing temperature and work hardening lead to decreased wear performance as the cutting speed increases.

These results agree with the onset and evolution of wear modes observed in turning tests at 50 and 70 m/min. In fact the wear patterns observed for both configurations $\kappa_r=0°$ and $\kappa_r=45°$ can be explained with the help of numerical modeling, showing much more aggressiveness for the cutting edge for configuration $\kappa_r=0°$. This condition corresponds to the onset and progression of chipping, notching and flank wear being the dominant wear modes.

Acknowledgments

The authors are indebted to the Ministry of Economy and Competitiveness of Spain for providing the financial support for this work (under Project DPI2008-06746)

References

[1] Ezugwu EO. Key improvements in the machining of difficult-to-cut aerospace superalloys. Int J Mach Tools Manuf 2005;45(12–13):1353–67.
[2] Bhatt A, Attia H, Vargas R, Thomson V. Wear mechanisms of WC coated and uncoated tools in finish turning of Inconel 718. Tribol Int 2010;43:1113–21.
[3] Devillez A, Schneider F, Dominiak S, Dudzinski D, Larrouquere D. Cutting forces and wear in dry machining of Inconel 718 with coated carbide tools. Wear 2007;262:931–42.
[4] Rossini NS, Dassisti M, Benyounis KY, Olabi AG. Methods of measuring residual stresses in components. Mater Des 2012;35:572–88.
[5] Pawade RS, Joshi SS, Brahmankar PK. Effect of machining parameters and cutting edge geometry on surface integrity of high-speed turned Inconel 718. Int J Mach Tools Manuf 2008:15–28.
[6] Courbon C, Pusavec F, Dumont F, Rech J, Kopac J. Tribological behavior of Ti6Al4V and Inconel718 under dry and cryogenic conditions—application to the context of machining with carbide tools. Tribol Int 2013;66:72–82.
[7] Zhu Dahu, Zhang Xiaoming, Ding Han. Tool wear characteristics in machining of nickel-based superalloys. Int J Mach Tools Manuf 2013;64:60–77.
[8] Lorentzon J, Järvstrat N. Modeling tool wear in cemented-carbide machining alloy 718. Int J Mach Tools Manuf 2008;48:1072–80.
[9] Aurich JC, Bil H. 3D finite element modeling of segmented chip formation. CIRP Ann – Manuf Technol 2006;55(1):47–50.
[10] Özel T. Computational modeling of 3D turning: influence of edge micro-geometry on forces, stresses, friction and tool wear in PCBN tooling. J Mater Process Technol 2009;209:5167–77.
[11] Ozel T, Sima M, Srivastava AK, Kaftanoglu B. Investigations on the effects of multi-layered coated inserts in machining Ti–6Al–4V alloy with experiments and finite element simulations. CIRP Ann – Manuf Technol 2010;59:77–82.
[12] Attanasio A, Ceretti E, Rizzuti S, Umbrello D, Micari F. 3D finite element analysis of tool wear in machining. CIRP Ann – Manuf Technol 2008;57:61–4.
[13] Özel T, Ulutan D. Prediction of machining induced residual stresses in turning of titanium and nickel based alloys with experiments and finite element simulations. CIRP Ann – Manuf Technol 2012;61:547–50.
[14] Rotella G, Dillon Jr. OW, Umbrello D, Settineri L, Jawahir IS. Finite element modeling of microstructural changes in turning of AA7075-T651 alloy. J Mater Process Technol 2013;15(1):87–95.
[15] Uhlmann E, Graf von der Schulenburg M, Zettier R. Finite element modeling and cutting simulation of Inconel 718. CIRP Ann – Manuf Technol 2007;56(1):61–64.
[16] Soo SL, Aspinwall DK, Dewes RC. 3D FE modeling of the cutting of Inconel 718. J Mater Process Technol 2004;150:116–23.
[17] Lazoglu I, Islam C. Modeling of 3D temperature fields for oblique machining. CIRP Ann – Manuf Technol 2012;61:127–30.
[18] Illoul L, Lorong P. On some aspects of the CNEM implementation in 3D in order to simulate high speed machining or shearing. Comput Struct 2011;89:940–58.
[19] Cantero JL, Díaz J, Miguélez H, Marín N. Analysis of tool wear patterns in finishing turning of Inconel 718. Wear 2013;297:885–94.
[20] Muñoz-Sánchez A, Canteli JA, Cantero JL, Miguélez MH. Numerical analysis of the tool wear effect in the machining induced residual stresses. Simul Model Pract Theory 2011;19:872–86.
[21] Filice L, Micari F, Settineri L, Umbrello D. Wear modeling in mild steel orthogonal cutting when using uncoated carbide tools. Wear 2007;262:545–54.
[22] Tounsi N, Attia H. Identification of Constitutive Law for Inconel 718 in Machining, HRC-CNRC, Report developed for SFTC. Deform 3D library (2007).
[23] Molinari A, Cheriguene R, Miguelez H. Numerical and analytical modeling of orthogonal cutting: the link between local variables and global contact characteristics. Int J Mech Sci 2011;53:183–206.
[24] Molinari A, Cheriguene R, Miguélez M H. Contact variables and thermal effects at the tool–chip interface in orthogonal cutting. Int J Solids Struct 2012;49:3774–96.
[25] Özel T, Ulutan D. Prediction of machining induced residual stresses in turning of titanium and nickel based alloys with experiments and finite element simulations. CIRP Ann – Manuf Technol 2012;61:547–50.
[26] Grzesik W, Nieslony P. A computational approach to evaluate temperature and heat partition in machining with multilayer coated tools. Int J Mach Tools Manuf 2003;43:1311–7.
[27] Turning Catalogue, Seco Tools, 2009.
[28] Olovsjö S, Nyborg L. Influence of microstructure on wear behavior of uncoated WC tools in turning of Alloy 718 and Waspaloy. Wear 2012;282–283:12–21.
[29] Miguélez MH, Soldani X, Molinari A. Analysis of adiabatic shear banding in orthogonal cutting of Ti alloy. Int J Mech Sci 2013;75:212–22.
[30] Haddag B, Nouari M. Tool wear and heat transfer analyses in dry machining based on multi-steps numerical modeling and experimental validation. Wear 2013;302:1158–70.
[31] Deshpande A, Madhavan V. A novel approach to accelerate attainment of thermal steady state in coupled thermomechanical analysis of machining. Int J Heat Mass Transf 2012;55:3869–84.
[32] Toropov A, Ko S-L. Prediction of tool-chip contact length using a new slip-line solution for orthogonal cutting. Int J Mach Tools Manuf 2003;43:1209–15.